Journal of Alloys and Compounds 513 (2012) 552–558

Contents lists available at SciVerse ScienceDirect

Journal of Alloys and Compounds

journal homepage: www.elsevier.com/locate/jallcom

Liquid phase deposition (LPD) of TiO_2 thin films as photoanodes for cathodic protection of stainless steel

C.X. Lei [a], H. Zhou [a], Z.D. Feng [a,*], Y.F. Zhu [b], R.G. Du [b,**]

[a] College of Materials, Xiamen University, Xiamen 361005, China
[b] College of Chemistry and Chemical Engineering, Xiamen University, Xiamen 361005, China

ARTICLE INFO

Article history:
Received 17 May 2011
Received in revised form 1 November 2011
Accepted 2 November 2011
Available online 9 November 2011

Keywords:
Liquid phase deposition
TiO_2 thin film
Photoanode
Cathodic protection

ABSTRACT

In this paper, the liquid phase deposition (LPD) technique was developed to prepare TiO_2 thin films on ITO conducting glass applied to the photogenerated cathodic protection of SUS304 stainless steel (304SS). The results showed that a dense and crack-free anatase TiO_2 film with a thickness of 800 nm was prepared from the LPD process at 80 °C for 3 h. Moreover, the TiO_2 films exhibited a decrease in crystal preferential orientation and an increase in optical band gap energy when heat treated at 300 °C and 500 °C. In addition, the results of the photoelectrochemical measurements showed that the photopotential of the as-deposited TiO_2 film was stabilized at about −200 mV, whereas those of the films subjected to heat treatment at 300 °C and 500 °C were stabilized at −400 mV and −460 mV, respectively. It was indicated that both the as-deposited and the heat treated LPD-derived TiO_2 films exhibited sufficiently negative electrode potential under illumination, which could serve as the photoanodes for effective cathodic protection of 304SS.

1. Introduction

The corrosion prevention of metals or steels has been widely investigated by many researchers all over the world. The traditional methods applied to the anticorrosion of metals are the sacrificial anode [1] and impressed current [2] cathodic protection, as well as the barrier layer protection using the organic or ceramic coatings to separate the metals from the around environment [3–5]. However, the above methods cannot provide a long-standing protection for the metals due to the limited life-time of the applied materials and energy.

Recently, the application of TiO_2 semiconductor films to the photogenerated cathodic protection of metals is recognized as a sustainable anticorrosion method and is well developed by many researchers. In 1995, Yuan and Tsujikawa [6] have firstly proposed the concept of photogenerated cathodic protection. They discovered that the potential of TiO_2-coated copper substrate showed a negative shift under illumination. Accordingly, Fujishima and coworkers [7] have also reported that the TiO_2-coated stainless steel could also show a significant anticorrosion effect under the UV illumination. Inspired by these studies, Park et al. [8,9] have developed a novel photoelectrochemical approach for metal corrosion prevention using the TiO_2 semiconductor photoanode coupled with the stainless steel substrate. Since then, the preparation of TiO_2 photoanodes applied to the cathodic protection of stainless steels has attracted many researchers. Subasri et al. [10] have demonstrated that the effective cathodic protection of copper could be achieved by the sol-gel-derived TiO_2-based photoanodes. Using the titanium foils as substrates, both the anodization and hydrothermal technique were developed to prepare the TiO_2 nanotubes [11–13] as well as the net-like [14] and flower-like [15] TiO_2 films served as photoanodes for the cathodic protection of stainless steel. However, a relatively higher temperature (above 450 °C) heat treatment process is usually necessary for the above methods to prepare the anatase TiO_2 films, which would lead to some unfavorable changes on the microstructure and composition of the underlying substrates. Therefore, the development of low-temperature deposition of anatase TiO_2 films served as photoanodes is urgently required.

Liquid phase deposition (LPD) is a method that can obtain crystalline metal oxide films directly from aqueous solutions at low temperatures (25–100 °C) [16–18]. It is based on the slowly hydrolysis of metal fluoride complex $[MF_n]^{m-n}$ with the boric acid as the common fluorine scavenger [16]. The synthesis of TiO_2 films for photocatalysis application by means of LPD method was firstly reported by Deki and co-workers [19,20]. Since then, the LPD method has got attractive attentions due to its great advantages that require neither special equipment nor high energy supply [21–24]. However, to our best knowledge, few studies have carried out the researches on photogenerated cathodic protection of

* Corresponding author. Tel.: +86 0592 2181538; fax: +86 0592 2183937.
** Corresponding author. Tel.: +86 0592 2189192; fax: +86 0592 2186657.
E-mail addresses: zdfeng@xmu.edu.cn (Z.D. Feng), rgdu@xmu.edu.cn (R.G. Du).

0925-8388/$ – see front matter © 2011 Elsevier B.V. All rights reserved.
doi:10.1016/j.jallcom.2011.11.005

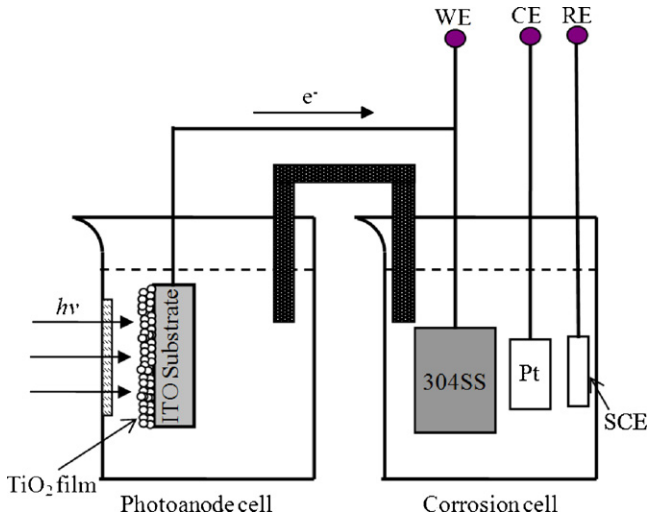

Fig. 1. Schematic illustration of the experimental device for photoelectrochemical measurements.

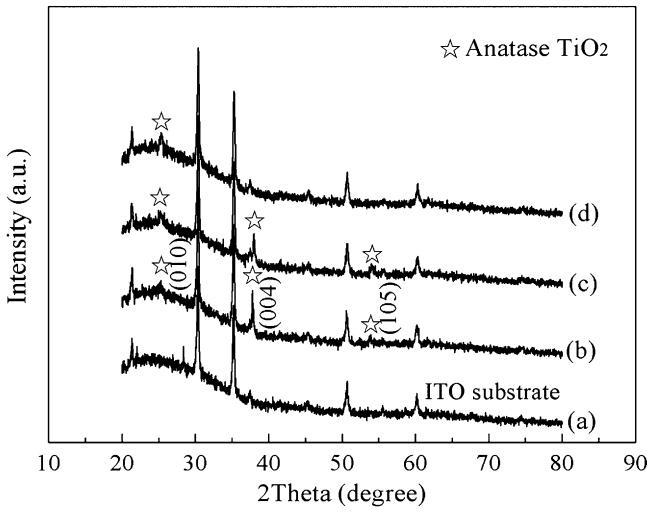

Fig. 3. XRD patterns of the LPD-derived films with heat treatment at different temperatures: (a) ITO substrate; (b) as-deposited film; (c) 300 °C-HT film; (d) 500 °C-HT film.

metals provided by the liquid phase deposited TiO_2 films. In this study, the LPD method was developed to prepare TiO_2 thin films on ITO conducting glass applied to the photogenerated cathodic protection of 304SS. The results showed that the dense and crack-free TiO_2 films with an effective photogenerated cathodic protection of 304SS were obtained. The photogenerated cathodic protection properties were further improved when the as-deposited films were heat treated at 300 °C and 500 °C. Moreover, under the illumination by the white light, the LPD-derived TiO_2 film without heat treatment could also provide a sufficiently negative electrode potential (−200 mV) for the cathodic protection of 304SS, which would exhibit a better promising application to the corrosion prevention.

2. Experimental details

2.1. Liquid phase deposition of TiO_2 films

The substrates used for liquid phase deposition in this study were ITO (In_2O_3:Sn) conducting glass (10 mm × 30 mm × 1 mm). Before the LPD experiments, the ITO glasses were ultrasonically cleaned in the acetone, ethanol and de-ionized water for 15 min, respectively. The precursor bath solutions were prepared by mixing 0.02 M $(NH_4)_2TiF_6$ and 0.06 M H_3BO_3 at the same volume (75 ml). The pH of the above mixed solution was kept at a natural value (pH 3.73) without further adjustment. During the LPD experiment, the cleaned ITO substrates were placed vertically into the precursor solutions, and the whole system was kept at 80 °C for 3 h. After the film deposition, the specimens were gently washed and naturally dried in the air. For comparison, some specimens were chosen to be annealed at 300 °C and 500 °C in the air for 3 h, with a heating rate of 5 °C/min.

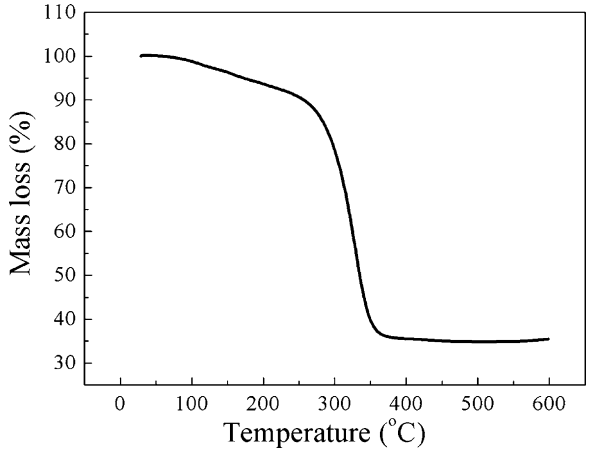

Fig. 2. The thermogravimetry (TG) curve of the as-deposited TiO_2 powders obtained from the LPD process.

2.2. Characterizations of the TiO_2 films

The phase structure of LPD-derived films on ITO substrates was identified by X'pert X-ray diffractometer (XRD, X'pert PRO, Panalytical, Netherlands) using CuKα_1 radiation (λ = 1.54056 Å) at 40 kV and 30 mA, with 2-theta ranged from 20° to 80°. The surface and cross section morphologies of the films were observed using scanning electron microscopy (FE-SEM, LEO1530). The Ultraviolet–visible (UV–vis) spectra of the films on ITO substrates were collected using an UV–vis spectrophotometer (Cary 50 Bio, Varian) by a transmittance mode. The thermogravimetry (TG) measurement of the LPD-derived TiO_2 powder was performed using a TG-DTA instrument (Thermische Analyse, NETZSCH), under an air atmosphere with a heating rate of 10 °C/min from room temperature to 600 °C. The surface chemical composition analysis of LPD-derived films was performed using X-ray photoelectron spectroscopy (XPS, PHI Quantum 2000) with an Al-Kα radiation source. All of the specimens were subjected to Ar etching of 30 nm from the top-surface before the data collection during the XPS measurements. The binding energies were normalized to the signal for adventitious carbon at 284.8 eV.

2.3. Photoelectrochemical measurements

The schematic illustration of the experimental device for photoelectrochemical measurements was shown in Fig. 1. The measurements were performed using Model 263A potentiostat/galvanostat (EG&G Instruments, Inc., USA, Princeton Applied Research) connected to a SBP300 grating spectrometer with a LPX 150 W Xe lamp as the illumination source [11–15]. During the photoelectrochemical measurements, a polytetrafluoroethene (PTFE) container with a quartz window to transmit the light was used as the photoelectrochemical cell. The SUS304 stainless steel (10 mm × 30 mm × 1 mm) foils used in this study were mechanically polished to a mirror finish with Al_2O_3 suspension solution, and then ultrasonically cleaned in acetone, ethanol and de-ionized water, respectively. Both the TiO_2/ITO electrode and the polished 304SS electrode were prepared with an active area of 1 cm^2. The back and edges of the electrodes were all covered with 704 silicone rubber to expose only the front active surface to the electrolyte solution. The TiO_2/ITO electrode was served as a photoanode in the photoelectrochemical cell while the coupled 304SS electrode as the working electrode in the corrosion cell. Moreover, the saturated calomel electrode (SCE) was served as the reference electrode while platinum foils as the counter electrode. The electrolyte used in the photoelectrochemical cell was 0.05 M sodium formate solution [9], while in the corrosion cell was 0.5 M NaCl solution. The open circuit potentials (OCP) of the coupled electrodes were measured under illumination by intermittent white light (with the wavelength ranging from 250 nm to 700 nm). During the measurements of photocurrent spectra, an M5210 lock-in amplifier/chopper setup (with a chopper frequency of 34 Hz) were used and connected to the above electrochemical working station. All of the photocurrent curves of the LPD-derived TiO_2 photoanodes were collected under the illumination without the application of bias voltages.

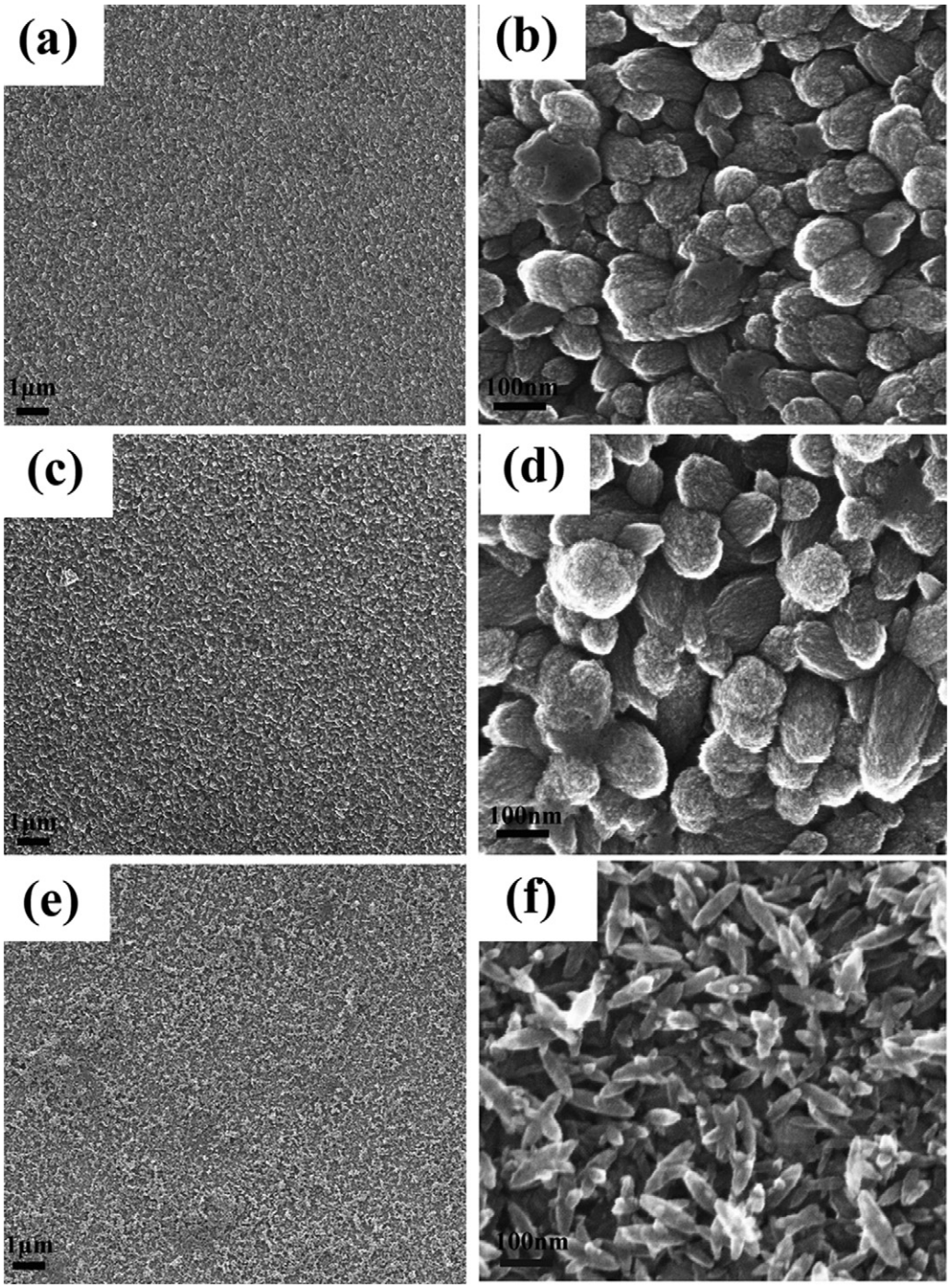

Fig. 4. Surface morphologies of the TiO_2 thin films with heat treatment at different temperatures: (a and b) as-deposited film; (c and d) 300 °C-HT film; (e and f) 500 °C-HT film.

3. Results and discussion

3.1. Thermal analysis

The thermogravimetry (TG) curve of the as-deposited TiO_2 powder obtained from the LPD process is shown in Fig. 2. This curve could be divided into three stages. The first stage was observed with the temperature ranging from the room temperature to 260 °C, with the mass loss of about 10.3%, which was mainly attributed to the evaporation of physically absorbed water. The temperature ranging from 260 °C to 380 °C was assigned as the second stage, and the largest mass loss of about 53.9% was found. This stage was associated with the thermal decomposition of some immediate compounds containing NH_4^+ and F^- in the LPD-derived TiO_2 powders [16]. In general, the process of liquid phase deposition of anatase TiO_2 was performed through the following reactions [25,26]:

$$TiF_6^{2-} \xrightarrow{nOH^-} TiF_{6-n}(OH)_n^{2-} + nF^- \xrightarrow{(6-n)OH^-} Ti(OH)_6^{2-} + 6F^-$$

$$BO_3^{3-} + 4F^- + 6H^+ \rightarrow BF_4^- + 3H_2O$$

$$Ti(OH)_6^{2-} \xrightarrow{H_2O} TiO_2$$

It was indicated that the intermediate phases such as $(NH_4)_2TiF_{6-n}(OH)_n$ cannot be completely ruled out in the

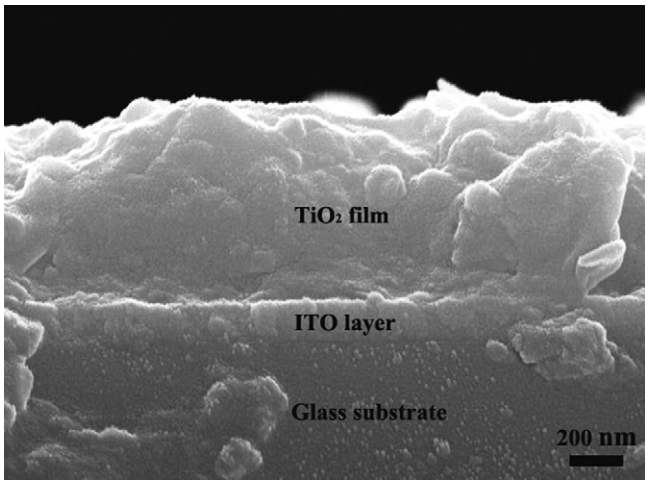

Fig. 5. The cross section morphology of the as-deposited TiO_2 film on ITO substrate by LPD method.

as-prepared TiO_2 powders or films. In addition, the previous study also reported that the LPD-derived TiO_2 always contained nitrogen and fluorine elements, and these impurities could be significantly decomposed upon calcination above 300 °C [20]. In the present study, the significant mass loss was observed in the second stage between 260 °C and 380 °C, which would be mainly caused by the decomposition of the nitrogen and fluorine impurities. The temperature of the third stage was ranging from 380 °C to 600 °C, where the mass loss was only about 0.3%. This could be due to the dehydration and evaporation of the chemisorbed water.

3.2. XRD, SEM and XPS analysis

The XRD patterns of LPD-derived films on ITO substrates subjected to heat treatment (HT) at different temperatures are shown in Fig. 3. The small peak located at 2θ of 25.2° was observed for each coated sample (Fig. 3(b–d)), which was assigned as the anatase (PDF No. 21-1272) plane (0 1 0). It should be pointed out that the peak corresponding to anatase plane (0 0 4) with 2θ of 37.8° was difficult to resolve from the ITO substrate signal (peak with 2θ of 37.4°). However, compared to the blank ITO substrate, the intensity of the peak at 37.8° was strengthened for the TiO_2 coated ITO substrates, which was due to the contribution of the anatase TiO_2 thin film. This was also agreed well with the previous results about the LPD-derived TiO_2 films [27]. However, for the 500 °C-HT film, the intensity of (0 0 4) peak was relatively weaker. This implied that the higher temperature heat treatment process might inhibit the growth of anatase crystals along [0 0 1] direction. The previous study demonstrated that the anions such as F^-, BO_3^{3-}, BF_4^-, and TiF_6^{2-} included in the LPD precursor solution would adsorb to the surfaces parallel to the c axis of the TiO_2 crystals and inhibit the growth in the direction perpendicular to the c axis [28]. In that case, the anatase crystals would grow along the c-axis direction [28]. Therefore, the similar case would occur in this study. The impurities in the as-prepared TiO_2 films could result in a relatively strong (0 0 4) peak at 37.8°. Therefore, compared to the TiO_2 film without heat treatment, the intensity of (0 0 4) plane at 37.8° decreased for the 300 °C-HT sample and almost vanished for the 500 °C-HT sample, as the impurities were decomposed upon calcination.

The surface and cross section morphologies of the LPD-derived TiO_2 films on ITO substrates are shown in Figs. 4 and 5, respectively. The deposition of TiO_2 films on ITO conducting glass from aqueous solutions are favored due to the structural similarities between both semiconductor materials (the ITO layer and TiO_2 films) [27]. Consequently, the coherent and dense TiO_2 films could be readily formed on ITO substrates. In this study, the uniform and crack-free TiO_2 films with a thickness of 800 nm were obtained (Figs. 4 and 5). The as-deposited TiO_2 film exhibited a similar morphology to that of the 300 °C-HT sample. However, the 500 °C-HT TiO_2 film showed rather a different morphology, and large amounts of shuttle-like crystals were observed. Most of the TiO_2 crystals in the No-HT and 300 °C-HT films were perpendicular to the substrate, which indicated that certain preferential orientation was maintained in these films. Nevertheless, the crystals in the 500 °C-HT film were not orientated. This was also agreed well with the results obtained from the XRD analysis. It is known that the intermediate compounds which contained nitrogen and fluorine elements would significantly decomposed upon calcination at 500 °C [20]. Therefore, the crystals in 500 °C-HT films showed rather a random orientation as the impurities of the anions that resulted in the preferential orientation of TiO_2 crystals were significantly decomposed.

Fig. 6 shows the high-resolution XPS spectra of the Ti2p and O1s regions for the as-deposited and the heat-treated TiO_2 films obtained by the LPD process. It was observed that the Ti2p peaks of the 500 °C-HT film were shifted to a lower binding energy than those of the as-deposited and the 300 °C-HT films. This suggested that the 500 °C-HT film showed significant differences in the nanocrystalline structure of TiO_2 [29]. It was also confirmed by the XRD and SEM analysis, as significant differences in orientation and morphology were observed for TiO_2 nanocrystals in the 500 °C-HT film. The O1s bands of the LPD-TiO_2 films were deconvoluted using the symmetric Gaussian curves. The O1s peak was decomposed into two contributions for all the samples. The peak located at about 530.2 eV was attributed to the Ti–O in anatase TiO_2, whereas the peak at about 532.3 eV was assigned as the OH group in Ti–OH [25,30]. It was found that the peak area of anatase TiO_2 was greater than that of the Ti–OH after the sample was subjected to heat treatment at 300 °C and 500 °C. As the LPD samples were heat treated, the Ti–OH group in the as-deposited films would be completely converted into anatase TiO_2 according to the following reaction [25]:

$$\text{Ti–OH} + \text{OH–Ti} \rightarrow \text{Ti–O–Ti} + H_2O$$

Therefore, the heat treatment process would result in the more completely conversion of Ti–OH into anatase TiO_2.

3.3. UV–vis analysis

The UV–vis transmittance spectra of the as-deposited and heat-treated TiO_2 films on ITO substrates are shown in Fig. 7(a). The transmittance below 400 nm significantly decreased for all samples, which was attributed to the absorption of UV light caused by the jump of excited electrons from valance band to conduction band of TiO_2 films. The transmittance of the 500 °C-HT TiO_2 film was about 90% in the visible light and was significantly higher than that of the as-deposited and the 300 °C-HT TiO_2 films. This could be due to the smaller crystalline particles with only 30–40 nm in diameter on the surface of the 500 °C-HT TiO_2 film. With increasing heat treatment temperature, the absorption edge was shifted to a lower wavelength, which indicated that the band gap of TiO_2 films increased upon heat treatment. In order to obtain the quantitative estimate of the absorption edge of TiO_2 films, band gap energies of TiO_2 films in the present study could be calculated according to the following relation [31]:

$$(\alpha h\nu)^{1/2} = A(h\nu - E_g)$$

where α is the absorption coefficient of TiO_2 thin film, $h\nu$ is the photo energy, E_g is the optical band gap of thin film, and A is a constant that does not depend on photo energy. The intercepts of the tangents to the $\alpha^{1/2}$ versus photo energy ($h\nu$) would give

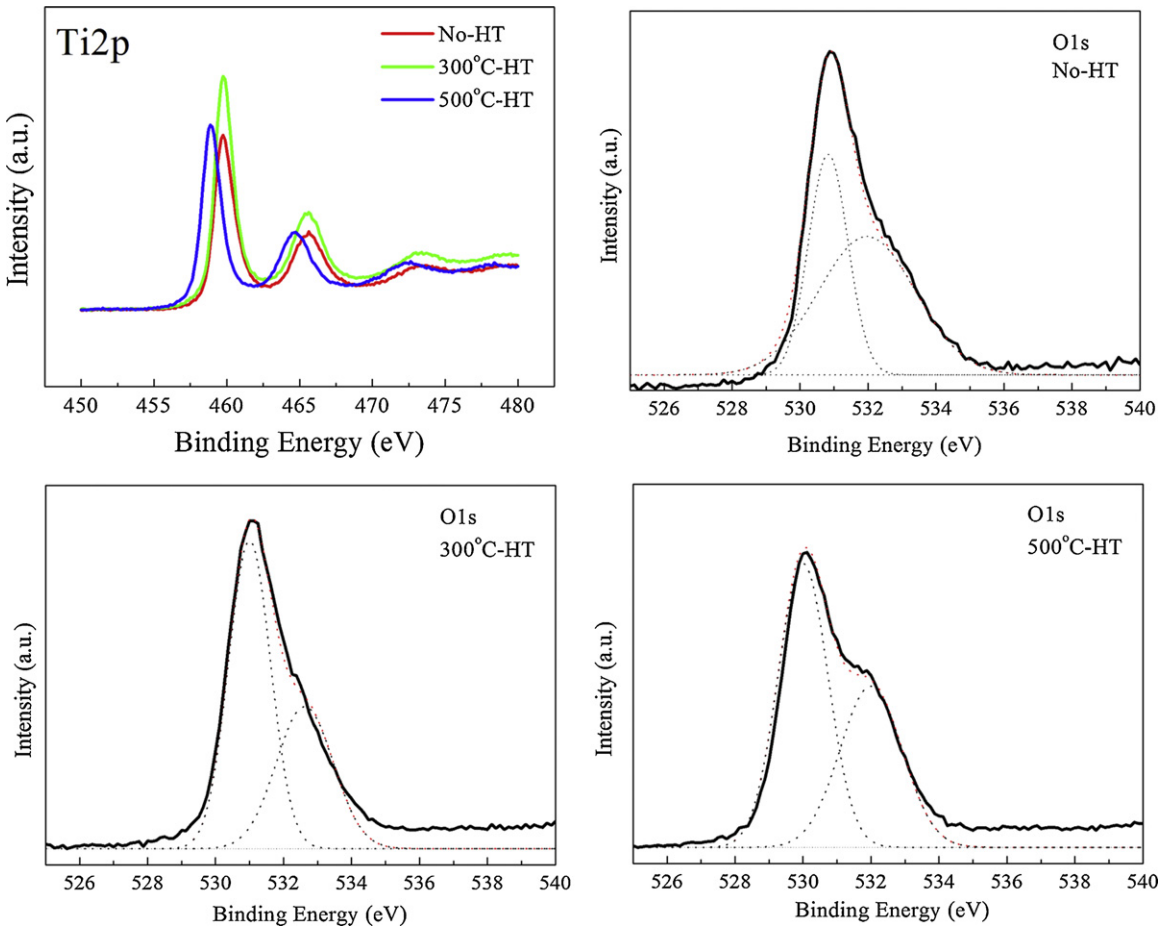

Fig. 6. The high-resolution XPS spectra of the Ti2p and O1s regions for the as-deposited and heat-treated TiO_2 films by LPD process.

an estimate of the optical band gap energies of TiO_2 thin films. Fig. 7(b) shows the plots of $\alpha^{1/2}$ versus photo energy ($h\nu$) for the as-deposited, 300 °C-HT and 500 °C-HT TiO_2 thin films, respectively. The band gap energies for the as-deposited, 300 °C-HT and 500 °C-HT TiO_2 films were estimated to be 2.98 eV, 3.08 eV, and 3.18 eV, respectively. These results also indicated that the band gap energies of LPD-TiO_2 films increased with increasing of the heat treatment temperature.

3.4. Photoelectrochemical performances

Fig. 8 shows the open circuit potential (OCP) changes for the coupled electrodes between TiO_2 films and 304SS under illumination by intermittent white light (with the wavelength ranging from 250 nm to 700 nm). It was observed that both the as-deposited and heat-treated samples exhibited a typical instantaneous n-type photoeffect under illumination. The open circuit potential (OCP) of each coupled electrode was rapidly shifted to a more negative value when the light was on. The stable value of the OCP under illumination was recorded as photopotential. It was found that the photopotential of the coupled electrode corresponding to the as-deposited TiO_2 film was stabilized at about −200 mV, whereas those of the 300 °C-HT and 500 °C-HT films were stabilized at −400 mV and −460 mV, respectively. Fig. 9 presents the photocurrent spectra for the as-deposited and 500 °C-HT TiO_2 films under illumination. A photocurrent peak located at about 325 nm was observed for the as-deposited TiO_2 films. The 500 °C-HT TiO_2 film exhibited a more broaden and intensive photocurrent peak, with the maximum photocurrent value of 492.7 nA located at 325 nm.

In this study, the white light with a wavelength ranging from 250 nm to 700 nm was used as the simulated sunlight. When the LPD-derived TiO_2 films were illuminated by the white light, the electron–hole pairs are generated in the TiO_2 layer. Driving by the electric field of the space-charge layer in TiO_2 semiconductor, the photogenerated holes would migrated to the electrolyte solution reacting with water and sodium formate according to the following equations [9,32]:

$$H_2O+2h^+ \rightarrow \frac{1}{2}O_2+2H^+ \quad (1)$$

$$h^+ + HCOO^- \rightarrow HCOO^\bullet \quad (2)$$

$$HCOO^\bullet \rightarrow CO_2 + H^+ + e^- \quad (3)$$

The electrons would transfer to the coupled 304SS electrode to lower its potential or react with the protons or water as following [32]:

$$2H^+ + e^- \rightarrow H_2 \quad (4)$$

$$\frac{1}{2}O_2+2e^-+H_2O \rightarrow 2OH^- \quad (5)$$

Therefore, the photopotential of the coupled electrodes under aerated conditions was determined both by the anodic photocurrent, as well as the cathodic current caused by the H^+ and O_2 reduction. The heat treatment process of LPD-derived TiO_2 films in the present study would result in a better crystallinity of the anatase TiO_2, which would allow the photogenerated electrons move faster in the TiO_2 layer. In that case, the possibility of the H^+ and O_2 reduction was largely inhibited, which gave rise to the more negative OCP and stronger intensity of anodic photocurrent. Nevertheless,

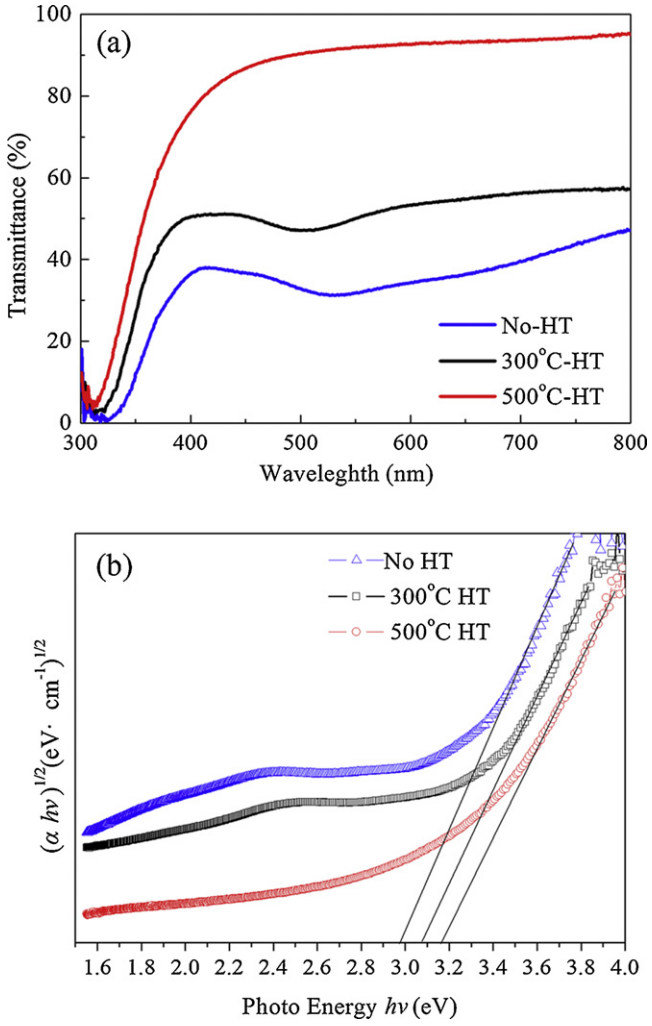

Fig. 7. The UV–vis transmittance spectra (a) and optical band gap (b) of the as-deposited and heat-treated TiO_2 films on ITO substrates by LPD process.

the as-deposited TiO_2 films also exhibited the sufficiently negative electrode potential (−200 mV), which was more negative than the corrosion potential of the bare 304SS (55 mV). This suggested that the photogenerated cathodic protection of 304SS was also achieved through the LPD-derived TiO_2 films even without the further heat

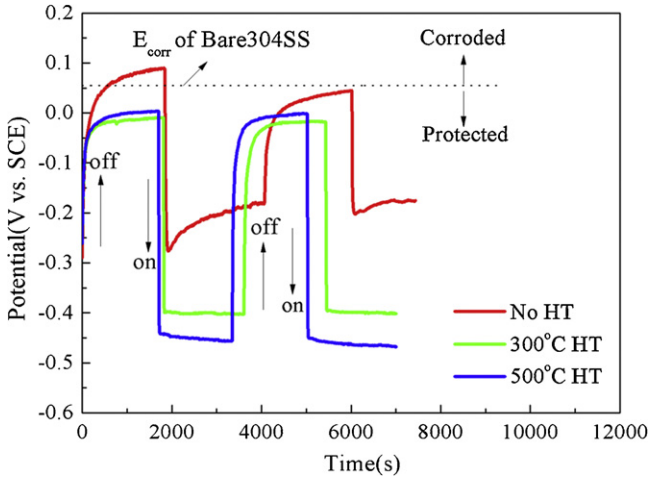

Fig. 8. The open circuit potential (OCP) changes for the coupled TiO_2/ITO and 304SS electrodes under illumination by intermittent white light (250 nm < λ < 700 nm).

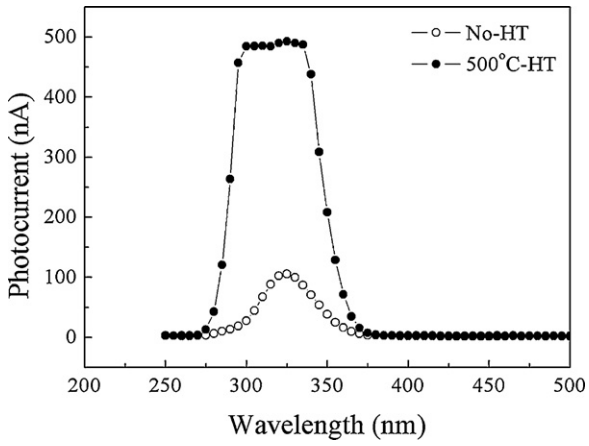

Fig. 9. The photocurrent spectra of the coupled TiO_2/ITO and 304SS electrodes under illumination.

treatment process. Therefore, the LPD-derived TiO_2 films would have great advantages in the application to the photogenerated cathodic protection of the substrates that could not be resistant to high temperature.

3.5. Analysis of photogenerated cathodic protection properties

When the LPD-derived anatase TiO_2 coated ITO electrode was contacted with the electrolyte solution (0.05 M sodium formate in this study), the thermodynamic equilibrium would take place at the interface between TiO_2 semiconductor and the electrolyte solution. Subsequently, a space-charged layer was formed at the surface layer of TiO_2 films. The potential difference in the space-charged layer would cause the band energy in the surface layer of TiO_2 films bend upwards. Therefore, when under illumination, the photogenerated electrons and holes would be separated in the space-charged layer, with the electrons moving toward the bulk TiO_2 films and the holes moving toward the interface of solid/solution. In that case, the degree of bending in the TiO_2 surface band energy decreased, and the photopotential was generated. It was reported that the thickness of space-charged layer in the surface of TiO_2 films would significantly influence the photoelectrochemical properties [33]. For the LPD-derived TiO_2 films in this study, the as-deposited TiO_2 films had a relatively thicker space-charged layer when immersed into the electrolyte solution, which would inhibit the movements of photogenerated electrons and holes. Therefore, the as-deposited TiO_2 films showed a less negative OCP and a lower photocurrent under illumination. By contrast, for the heat treated LPD-derived TiO_2 samples, the thickness of the TiO_2 films would decrease due to the decomposition of some intermediate compounds during the heat treatment process, and a thinner space-charged layer would be generated in the surface of heat-treated TiO_2 films. In that case, the photogenerated electrons could move fast in the thinner space-charged layer. Moreover, the higher crystallinity and less surface defects of the heat-treated TiO_2 films would also facilitate the movement of photogenerated electrons. Consequently, the more negative OCP and higher photocurrent were observed in the heat treated LPD-derived films, and the better photogenerated cathodic protection of 304SS was achieved.

4. Conclusions

The dense and crack-free TiO_2 thin films with a thickness of 800 nm on ITO substrates were successfully prepared by LPD method in this study. The heat treatment temperature had a significant effect on the structure and morphology of the TiO_2 films. The

TiO_2 films exhibited a decrease in crystal preferential orientation and an increase in optical band gap energy after heat treatment at 300 °C and 500 °C. The heat treated samples showed a more effective photogenerated cathodic protection of 304SS due to the more completely conversion of intermediate compounds into the better crystalline anatase TiO_2 phase. However, the as-deposited TiO_2 films without further heating treatment would also provide an effective cathodic protection for the 304SS, with the photopotential of about −200 mV, which was more negative than the corrosion potential of 304SS. In summary, the LPD-derived TiO_2 thin films both with and without heat treatment could provide an effective photogenerated cathodic protection of 304SS under the white light illumination.

Acknowledgments

This work was supported by the National High Technology Research and Development Program of China (2009AA03Z327) and Scientific and Technological Innovation Flat of Fujian Province (2009J1009).

References

[1] J. Ma, J. Wen, J. Alloys Compd. 496 (2010) 110–115.
[2] C. Christodoulou, G. Glass, J. Webb, S. Austin, C. Goodier, Corros. Sci. 52 (2010) 2671.
[3] J.A. Hill, T. Markley, M. Forsyth, P.C. Howlett, B.R.W. Hinton, J. Alloys Compd. 509 (2011) 1683–1690.
[4] M.B. Gonzalez, S.B. Saidman, Corros. Sci. 53 (2011) 276–282.
[5] R. Selvaraj, M. Selvaraj, S.V.K. Yer, Prog. Org. Coat. 64 (2009) 454–459.
[6] J. Yuan, S. Tsujikawa, J. Electrochem. Soc. 142 (1995) 3444–3450.
[7] Y. Ohko, S. Saitob, T. Tatsuma, A. Fujishima, J. Electrochem. Soc. 148 (2001) B24–B28.
[8] H. Park, K.Y. Kim, W. Choi, Chem. Commun. (2001) 281.
[9] H. Park, K.Y. Kim, W. Choi, J. Phys. Chem. B 106 (2002) 4775–4781.
[10] R. Subasri, T. Shinohara, K. Mori, J. Electrochem. Soc. 152 (2005) B105–B110.
[11] J. Li, C.J. Lin, J.T. Li, Z.Q. Lin, Thin Solid Films 519 (2011) 5494–5502.
[12] Z.Q. Lin, Y.K. Lai, R.G. Hu, J. Li, R.G. Du, C.J. Lin, Electrochim. Acta 55 (2010) 8717–8723.
[13] J. Li, C.J. Lin, C.G. Lin, J. Electrochem. Soc. 158 (2011) C55–C62.
[14] H. Yun, C.J. Lin, J. Li, J.R. Wang, H.B. Chen, Appl. Surf. Sci. 255 (2008) 2113–2117.
[15] J. Li, C.J. Lin, Y.K. Lai, R.G. Du, Surf. Coat. Technol. 205 (2010) 557–564.
[16] T.P. Niesen, M.R. De Guire, J. Electroceram. 6 (2001) 169–207.
[17] H. Parikh, M.R. De Guire, J. Ceram. Soc. Jpn. 117 (2009) 228–235.
[18] P.H. Lei, M.J. Ding, Y.C. Lee, M.J. Chung, J. Alloys Compd. 509 (2011) 6152–6157.
[19] S. Deki, Y. Aoi, O. Hiroi, A. Kajinami, Chem. Lett. 43 (1996) 3–434.
[20] H. Kishimoto, K. Takahama, N. Hashimoto, Y. Aio, S. Deki, J. Mater. Chem. 8 (1998) 2019–2024.
[21] R. Fujita, M. Sakairi, T. Kikuchi, S. Nagata, Electrochim. Acta 56 (2011) 7180–7188.
[22] M.K. Lee, C.H. Fan, H.C. Wang, C.Y. Chang, J. Electrochem. Soc. 158 (2011) D511–D514.
[23] J. Wang, Z. Wang, H. Li, Y. Cui, Y. Du, J. Alloys Compd. 494 (2010) 372–377.
[24] Y.B. Ding, C.Z. Yang, L.H. Zhu, J.D. Zhang, J. Hazard. Mater. 175 (2010) 96–103.
[25] J.G. Yu, H.G. Yu, B. Cheng, X.J. Zhao, J.C. Yu, W.K. Ho, J. Phys. Chem. B 107 (2003) 13871–13879.
[26] Y. Masuda, S. Ieda, K. Koumoto, Langmuir 19 (2003) 4415–4419.
[27] D. Gutierrez-Tauste, X. Domenech, M.A. Hernandez-Fenollosa, J.A. Ayllón, J. Mater. Chem. 16 (2006) 2249–2255.
[28] Y. Masuda, T. Sugiyama, W.S. Seo, K. Koumoto, Chem. Mater. 15 (2003) 2469–2476.
[29] A.O.T. Patrocínio, E.B. Paniago, R.M. Paniago, N.Y.M. Paniago, Appl. Surf. Sci. 254 (2008) 1874–1879.
[30] D. Wu, M. Long, W. Cai, C. Chen, Y. Wu, J. Alloys Compd. 502 (2010) 289–294.
[31] B. Zhao, J. Zhou, Y. Chen, Y. Peng, J. Alloys Compd. 509 (2011) 4060–4064.
[32] R. Subasri, T. Shinohara, Electrochem. Commun. 5 (2003) 897–902.
[33] R. Subasri, T. Shinohara, Res. Chem. Intermed. 31 (2005) 275–283.